



Range dependence of an optical pulse position modulation link in the presence of background noise

WOJCIECH ZWOLIŃSKI,¹ MARCIN JARZYNA,^{2,*} AND KONRAD BANASZEK^{1,2}

¹*Faculty of Physics, University of Warsaw, Pasteura 5, PL-02-093 Warsaw, Poland*

²*Centre of New Technologies, University of Warsaw, Banacha 2c, PL-02-097 Warsaw, Poland*

*m.jarzyna@cent.uw.edu.pl

Abstract: We analyze the information efficiency of a deep-space optical communication link with background noise, employing the pulse position modulation (PPM) format and a direct-detection receiver based on Geiger-mode photon counting. The efficiency, quantified using Shannon mutual information, is optimized with respect to the PPM order under the constraint of a given average signal power in simple and complete decoding scenarios. We show that the use of complete decoding, which retrieves information from all combinations of detector photocounts occurring within one PPM frame, allows one to achieve information efficiency scaling as the inverse of the square of the distance, i.e. proportional to the received signal power. This represents a qualitative enhancement compared to simple decoding, which treats multiple photocounts within a single PPM frame as erasures and leads to inverse-quartic scaling with the distance. We provide easily computable formulas for the link performance in the limit of diminishing signal power.

© 2018 Optical Society of America under the terms of the [OSA Open Access Publishing Agreement](#)

1. Introduction

Optical domain offers numerous benefits for deep-space communication compared to the radio frequency band [1]. The primary advantage is access to a much wider bandwidth. Furthermore, the use of laser sources substantially reduces loss due to diffraction of the beam propagating through space, allowing for improved targeting of the emitted signal power. Other technical reasons, such as prospectively lesser in size and weight onboard transmitter modules and the absence of regulatory issues inherent to the use of the radio spectrum additionally make optical communication the technology of choice for future space missions. This motivates a careful study of the performance limits of optical communication links in the photon-starved regime typical for deep-space scenarios.

The standard approach to deep-space optical communication relies on the pulse position modulation (PPM) format shown schematically in Fig. 1(a) which encodes information in symbols defined by the position of a light pulse within a frame of otherwise empty time bins [2–4]. High photon efficiency is achieved by direct detection of the PPM symbols with the help of time-resolved photon counting. In the photon-starved regime some pulses may escape detection, resulting in lower than one probability to generate a click in the bin occupied by a pulse. In the absence of background noise this leads to erasures of input PPM symbols which can be efficiently dealt with using standard error correcting codes [5]. Remarkably, it can be shown that with diminishing average signal power the directly-detected PPM format optimized over the number of time bins within a frame attains the capacity of a narrowband bosonic channel [6] in the leading order of the power parameter [7–10]. This is associated with unboundedly growing photon information efficiency as the signal power goes to zero.

The above picture becomes much more nuanced when background noise is taken into account.

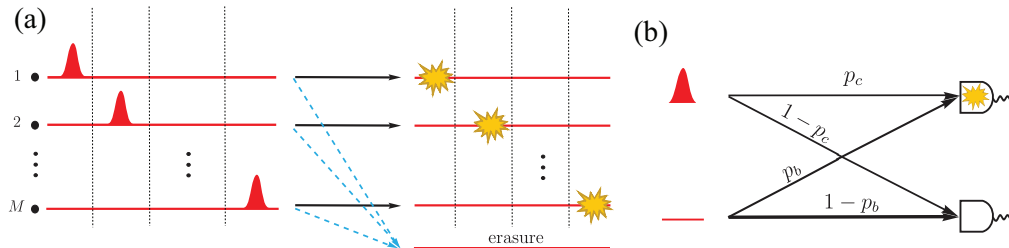


Fig. 1. (a) The PPM format uses M equiprobable symbols defined by the location of a light pulse in a frame of otherwise empty bins. In the noise-free scenario the input symbol is either identified unambiguously by the timing of the detector click, or erased. (b) In the presence of noise both a light pulse and an empty time bin can generate a detector click with respective probabilities p_c and p_b .

The common conviction is that in this case the maximum attainable transmission rate scales asymptotically as the inverse of the fourth power of the distance between the transmitter and the receiver [11, 12], corresponding to vanishing photon information efficiency. This is quadratically worse compared to coherent communication at radio frequencies, for which information rate exhibits inverse-square scaling with the distance in the power-limited regime. Such inverse-square scaling can be viewed as a result of photon information efficiency attaining a constant value, equal to 1 nat or 2 nats ($1 \text{ nat} \approx 1.44 \text{ bits}$) respectively for shot-noise limited heterodyne or homodyne detection as implied by the Shannon-Hartley theorem [13].

The purpose of this paper is to examine carefully using Shannon theory [14] the performance limits of an optical communication link based on the PPM format with direct detection in the presence of background noise. We consider a realistic model of Geiger-mode photon counting detectors which provide only a binary click or no-click outcome in an individual time bin. We demonstrate theoretically that under the constraint of a given average optical power such a system can in principle achieve inverse-square scaling with the distance while offering at the same time high photon information efficiency exceeding the Shannon-Hartley limit. Two ingredients necessary to achieve this regime of operation are identified. The first one is soft decoding strategy which retrieves information from all possible photocount patterns, including multiple clicks within one PPM frame. The second ingredient is the ability to implement the PPM format of an arbitrarily high order, with an unboundedly growing number of time bins within one frame. Under the average power constraint this implies unlimited pulse peak power used in the PPM format. Although this requirement may be incompatible with technical limitations of lasers used in onboard transmitters, we point out that the recently presented concept of structured optical receivers [15–17] enables one to achieve the performance equivalent to the PPM format with evenly distributed instantaneous power of the transmitted optical signal.

This paper is organized as follows. In Sec. 2 we review the relevant parameters of a communication link. The information rate is calculated in Sec. 3. The asymptotic analysis of the information rate in the limit of diminishing signal power is analyzed in Sec. 4. These results are used to discuss quantitatively the range dependence of an exemplary PPM link in Sec. 5. Finally, Sec. 6 concludes the paper.

2. System characteristics

The elementary parameters characterizing the transmitter are the optical power P_{tx} and the bandwidth B , which defines the duration of an individual time bin as $1/B$. Consequently, the average emitted photon number per time bin is $P_{\text{tx}}/(Bhf_c)$, where h is Planck's constant and f_c is the signal carrier frequency. Propagation losses and non-unit efficiency η_{det} of the detector reduce this figure in a linear manner, which yields the average detected signal photon number n_a per time bin given by

$$n_a = \eta_{\text{tot}} \frac{P_{\text{tx}}}{Bhf_c}, \quad \eta_{\text{tot}} = \eta_{\text{det}} \left(\frac{\pi f_c D_{\text{tx}} D_{\text{rx}}}{4cr} \right)^2. \quad (1)$$

In the above expression D_{tx} and D_{rx} are respectively the diameters of the transmitter and the receiver antennas, r is the distance covered by the optical link, and c denotes the speed of light. Conveniently, n_a is a dimensionless parameter characterizing the strength of the detected signal. Diffraction losses taken into account in Eq. (1) make n_a scale as r^{-2} with the range when all other parameters of the link are fixed. We will be interested in the photon-starved regime arising for large distances, when $n_a \ll 1$.

The M -ary PPM format uses M equiprobable symbols corresponding to the location of a single light pulse in a frame of M otherwise empty bins shown in Fig. 1(a). In order to satisfy the average power constraint, the mean photon number in the signal pulse needs to be equal to $n_s = Mn_a$. Without background noise, direct detection identifies unambiguously the input symbol through the timing information, unless the photon counting detector does not click at all over the duration of the PPM frame. According to the standard theory of photodetection [18] the probability of such an erasure event is $\exp(-n_s)$. From the information theoretic viewpoint the communication scheme is described by an M -ary erasure channel with the probability of faithful transmission equal to $1 - \exp(-n_s)$.

In the presence of background noise, photocounts may occur also in empty time bins. The noise model considered in this work is based on an assumption that stray light and dark counts generate background whose strength is equivalent to n_b photons per time bin and that background counts are statistically independent from each other as well as uncorrelated with the incoming signal. Furthermore, we will take a realistic model for photon counting which discriminates only between the presence or absence of clicks in a given time bin, which applies e.g. to avalanche photodiodes operated in the Geiger mode. Thus the detector generates a click in an empty time bin and a bin occupied by a light pulse with respective probabilities

$$p_b = 1 - \exp(-n_b), \quad p_c = 1 - \exp(-n_s - n_b). \quad (2)$$

The conditional probabilities for a single time bin are depicted schematically in Fig. 1(b). Other noise models, such as single-mode thermal fluctuations [19], can be analyzed by replacing Eq. (2) with suitable alternative expressions and following steps described below.

3. Information rate

The most elementary decoding strategy for a noisy link is to interpret as erasures all events when clicks have occurred in multiple time bins within one PPM frame. Such simple decoding would either recover the input PPM symbol, although with a certain error probability induced by background counts, or yield an erasure event. A more general soft decoding strategy is to retrieve information also from sequences containing multiple clicks in individual PPM frames. The maximum attainable transmission rate is given by the Shannon mutual information evaluated for output events taken into consideration. The probability of obtaining a sequence of k clicks in specific bins within one PPM frame is given by one of two expressions

$$p_c(k) = p_c p_b^{k-1} (1 - p_b)^{M-k}, \quad p_e(k) = (1 - p_c) p_b^k (1 - p_b)^{M-k-1} \quad (3)$$

depending respectively on whether the signal pulse was located in one of the time bins where a click has occurred or not. In the former case the pulse generates a click with a probability p_c and $k - 1$ clicks are produced by background noise in empty time bins, each with a probability p_b . The factor $(1 - p_b)^{M-k}$ stems from the fact that no click may occur in the remaining $M - k$ bins. In the latter case, all k clicks are generated by background noise present in empty time bins and the bin carrying a pulse does not produce a click, hence the factor $1 - p_c$. For a given value of k there are $\binom{M-1}{k-1}$ click sequences where a count has occurred in a time bin containing the light pulse and $\binom{M-1}{k}$ sequences where this was not the case. The marginal probability of observing a given sequence of k clicks for any of the M equiprobable input PPM symbols is given by a weighted sum

$$p(k) = \frac{k}{M} p_c(k) + \left(1 - \frac{k}{M}\right) p_e(k) \quad (4)$$

with the total number of sequences containing k clicks among M bins equal to $\binom{M}{k} = \binom{M-1}{k-1} + \binom{M-1}{k}$.

In order to take into account general soft decoding strategies, we will evaluate mutual information per time bin $I^{(K)}$ for a scenario when information is retrieved from sequences containing up to K clicks, while other events are interpreted as erasures. The complete expression reads:

$$I^{(K)} = \frac{1}{M} \sum_{k=1}^K \left[\binom{M-1}{k-1} p_c(k) \log_2 p_c(k) + \binom{M-1}{k} p_e(k) \log_2 p_e(k) - \binom{M}{k} p(k) \log_2 p(k) \right]. \quad (5)$$

The first two terms stem from the average conditional entropy of the output when the input symbol is known, whereas the last term is contributed by the entropy of the output variable itself. Simple decoding corresponds to the case $K = 1$, whereas for complete decoding $K = M$. In the following discussion it will be convenient to use as the figure of merit the photon information efficiency (PIE) given by the ratio $I^{(K)}/n_a$, which specifies the amount of transmitted information per one detected photon. Because of the symmetry properties of the channel considered here from the information theoretic viewpoint we restrict our attention to the case of equiprobable input PPM symbols.

In Fig. 2 we present contour plots of PIE as a function of the PPM order M and the detected signal power n_a for a fixed background noise power $n_b = 10^{-3}$. Decoding restricted at a fixed level exemplified with $K = 1, 2, 5$ is compared to the complete decoding scenario when $K = M$. The qualitative difference between these two cases is clearly seen. While for restricted decoding PIE tends to zero with $n_a \rightarrow 0$, complete decoding enables one to attain a non-zero asymptotic value of PIE with an appropriate choice of the PPM order. This advantage of complete decoding is associated with a divergent asymptotic behaviour of the optimal PPM order M^* with the vanishing signal power, shown in Fig. 2 with dashed lines.

In order to gain further insights into the performance of the complete decoding scenario, in Fig. 3 we plot the maximum attainable photon information efficiency PIE^* and the corresponding optimal pulse optical energy n_s^* given by

$$\text{PIE}^* = \max_M (I^{(M)}/n_a) = I^{(M^*)}/n_a, \quad n_s^* = M^* n_a \quad (6)$$

as a function of the average detected optical power n_a for several values of the background noise parameter n_b . It is seen that in the limit $n_a \rightarrow 0$, both PIE^* and n_s^* tend to constant values which depend on the background noise. The arrows shown in Fig. 3(a) indicate the asymptotic values of the PIE calculated using the method presented in Sec. 4. This method provides also the asymptotic values of n_s^* , indicated with arrows in the inset of Fig. 3(b). Consequently, in the asymptotic limit the optimal PPM order $M^* = n_s^*/n_a$ scales inversely with the detected optimal

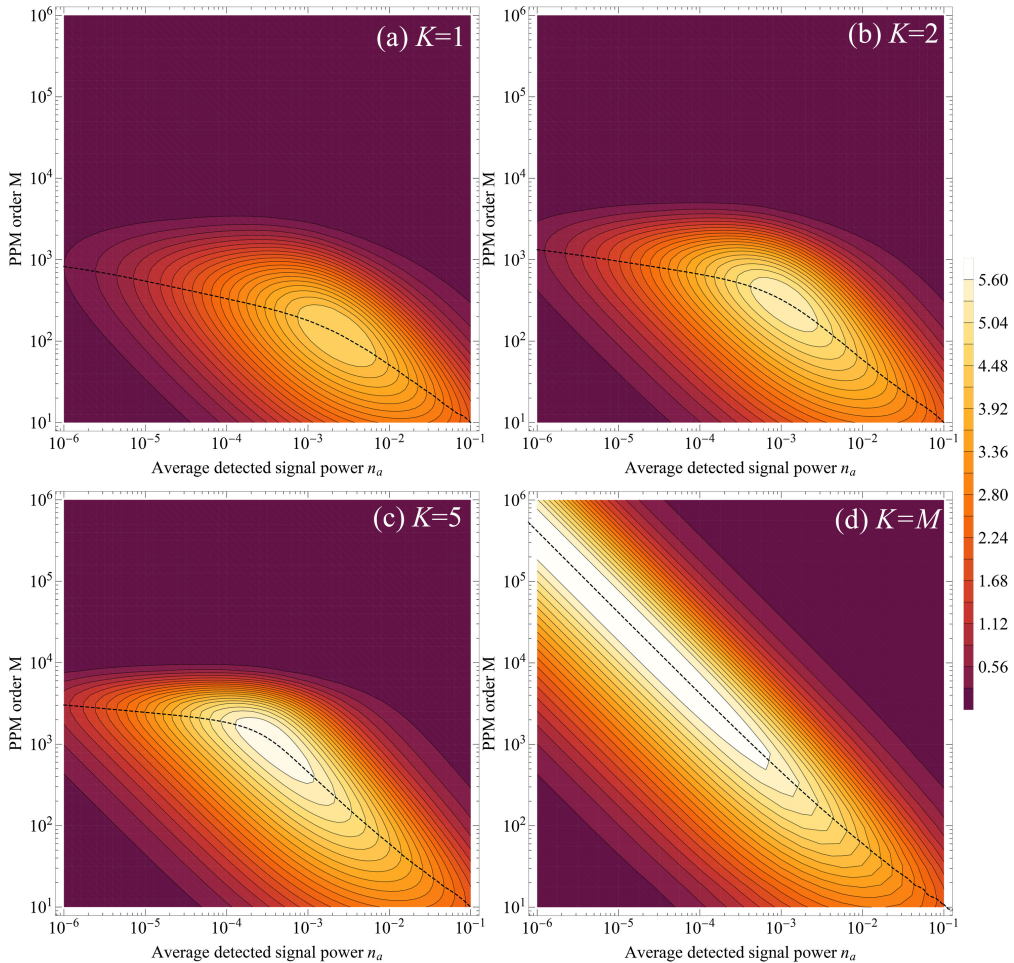


Fig. 2. Photon information efficiency $I^{(K)}/n_a$ as a function of the average detected signal power n_a and the PPM order M for a fixed background noise strength $n_b = 10^{-3}$. Results are shown for decoding restricted to sequences containing up to (a) $K = 1$, (b) $K = 2$, or (c) $K = 5$ clicks, as well as for (d) complete decoding with $K = M$. The dashed curves indicate the optimal PPM order M^* as a function of n_a .

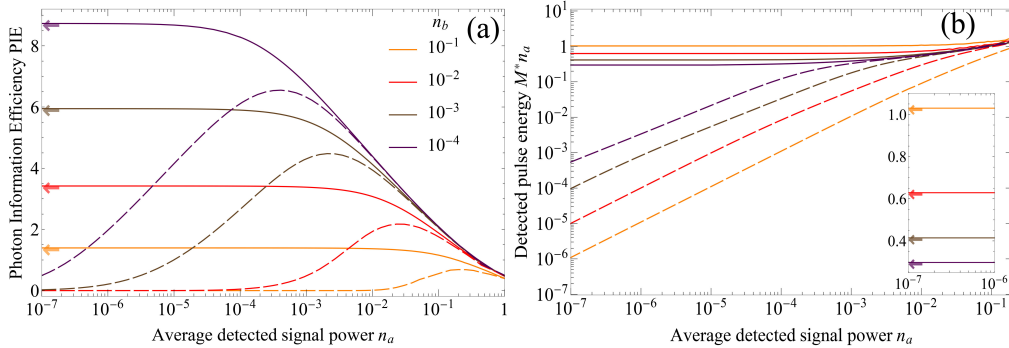


Fig. 3. (a) Photon information efficiency optimized over the PPM order for complete decoding $\text{PIE}^* = \max_M(I^{(M)}/n_a)$ (solid lines) and simple decoding $\max_M(I^{(1)}/n_a)$ (dashed lines), shown as a function of the average detected signal power n_a for several values of the background noise strength n_b . (b) The corresponding optimal pulse detected optical energy for complete decoding $n_s^* = M^*n_a$ (solid lines) and simple decoding (dashed lines). Arrows in the panel (a) and in the inset in the panel (b) indicate asymptotic values for the complete decoding scenario calculated using Eq. (9).

power n_a as seen in Fig. 2(d). The results for complete decoding are in stark contrast with the simple decoding strategy shown for comparison with dashed lines in Fig. 3. In the latter case, both the photon information efficiency and the optimal pulse energy tend to zero as $n_a \rightarrow 0$. On a side note, it is seen in Fig. 3(a) that the PPM format becomes photon inefficient for high optical powers. In this regime the PPM order is fixed and the probability p_c that the pulse generates a click approaches one.

4. Asymptotic PIE value

In this section we present a simple method to calculate the asymptotic values of the maximum photon information efficiency PIE^* and the corresponding optimal pulse optical energy n_s^* for the complete decoding scenario. The presented results are based on the information theoretic analysis of the channel capacity per unit cost [20]. The starting observation is that the M -ary PPM format can be viewed as a constrained version of generalized on-off keying (OOK) with a binary set of elementary symbols, where a light pulse is sent with a probability $1/M$ and an empty bin with the probability $1 - 1/M$. The constraint has the form of a requirement that every sequence of M consecutive time bins contains exactly one pulse. Because of this constraint, the mutual information $I^{(M)}$ for the completely-decoded PPM link is upper-bounded by the mutual information I_{OOK} for generalized OOK. The latter can be written as [14]

$$I^{(M)} \leq I_{\text{OOK}} = \left(1 - \frac{1}{M}\right) D\left(p_b || (1 - M^{-1})p_b + M^{-1}p_c\right) + \frac{1}{M} D\left(p_c || (1 - M^{-1})p_b + M^{-1}p_c\right) \quad (7)$$

where p_b and p_c are defined in Eq. (2) and

$$D(p||q) = p \log_2 \frac{p}{q} + (1-p) \log_2 \frac{1-p}{1-q} \quad (8)$$

denotes the relative entropy between binary probability distributions $(p, 1-p)$ and $(q, 1-q)$. Consequently, for a given n_a the photon information efficiency PIE^* for the PPM format optimized over the order M will be less or equal to $\text{PIE}_{\text{OOK}}^* = \max_M(I_{\text{OOK}}/n_a)$, where in the last expression maximization is carried out over M taken as a continuous positive parameter. Next, an upper

bound on $\text{PIE}_{\text{OOK}}^*$ can be obtained from the information theoretic result on the channel capacity per unit cost [20]. For the communication link analyzed here the cost is measured in terms of the optical energy and there is available exactly one input symbol whose cost is equal to zero, namely the empty time bin. In this setting the capacity per unit cost is monotone non-increasing in n_a and its asymptotic value PIE^{as} in the limit $n_a \rightarrow 0$ can be obtained from the following single-parameter maximization problem:

$$\text{PIE}^{\text{as}} = \max_{n_s \geq 0} \frac{D(p_c || p_b)}{n_s}, \quad (9)$$

where the ratio $D(p_c || p_b)/n_s$ on the right hand side of the above equation should be expressed using Eq. (2) in terms of two parameters: n_b , treated as a given constant, and n_s being the optimization variable.

The reasoning presented above implies that PIE^{as} defined in Eq. (9) specifies an upper bound on the photon information efficiency for the PPM format,

$$\text{PIE}^* \leq \text{PIE}_{\text{OOK}}^* \leq \text{PIE}^{\text{as}}. \quad (10)$$

Furthermore, we show in Appendix that the value PIE^{as} is actually attained in the limit $n_a \rightarrow 0$ by the photon information efficiency of an optimized PPM link in the complete decoding scenario. In Fig. 4 we plot PIE^{as} as a function of the background noise strength n_b . The figure also shows the optimal n_s^{as} maximizing the right hand side of Eq. (9). Let us recall that n_s^{as} specifies the *detected* optical energy of the pulse. The values PIE^{as} and n_s^{as} characterize the attainable long-range performance of a completely-decoded PPM link under a constraint of a fixed average detected signal power. This performance will be discussed in more detail in Sec. 5.

For completeness, we will close this section by analyzing the asymptotic limit $n_a \rightarrow 0$ of the simple decoding scenario. Fig. 3(b) indicates that in the case of simple decoding the optimal pulse energy n_s tends to zero with the diminishing average power n_a . This observation motivates expanding the mutual information $I^{(1)}$ into a power series in n_s . The leading order term has quadratic dependence on n_s ,

$$I^{(1)} \approx \log_2 e \frac{(M-1)e^{-(M-1)n_b}}{2M^2(1-e^{-n_b})} n_s^2. \quad (11)$$

Inserting $n_s = Mn_a$ yields the photon information efficiency for a given PPM order approximately equal to $I^{(1)}/n_a \approx (\log_2 e)(M-1)e^{-(M-1)n_b} n_a / [2(1-e^{-n_b})]$. With M treated as a continuous parameter, the right hand side of the above formula is maximized by $M = 1 + n_b^{-1}$, which gives:

$$\text{PIE}^{(1)} \approx \frac{\log_2 e}{2en_b(1-e^{-n_b})} n_a. \quad (12)$$

Thus the optimized photon information efficiency scales linearly with the average detected optical power n_a . This behavior is evidenced in Fig. 3(a) by the slope of the dashed curves. The corresponding optimal detected pulse energy, given approximately by

$$n_s^{(1)} \approx (1 + n_b^{-1})n_a \quad (13)$$

also exhibits asymptotic linear scaling in n_a , clearly seen in Fig. 3(b).

5. Range dependence

The maximum information rate R^* of a PPM link characterized by the bandwidth B can be written as:

$$R^* = B \cdot n_a \cdot \text{PIE}^*(n_a, n_b), \quad (14)$$

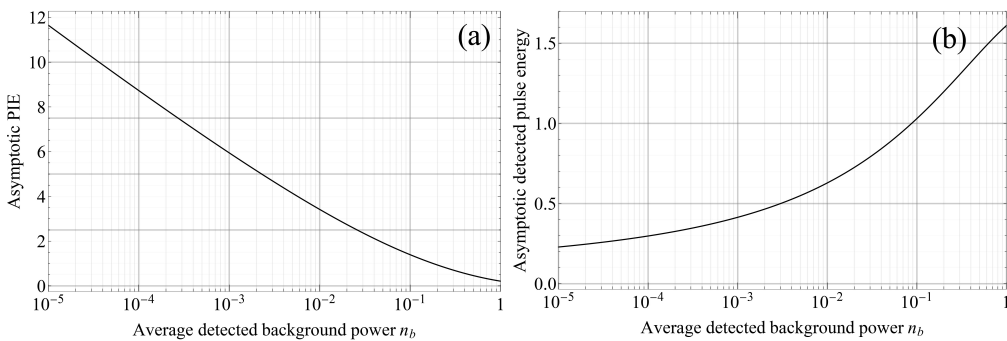


Fig. 4. (a) The asymptotic photon information efficiency PIE^{as} for a completely decoded PPM link in the limit of the vanishing average detected signal power $n_a \rightarrow 0$ as a function of the background noise strength n_b . (b) The corresponding optimal detected pulse energy n_s^{as} . The depicted values have been obtained using Eq. (9).

where n_a is the average detected signal power per time bin. For clarity, we explicitly stated here the dependence of the photon information efficiency PIE^* optimized with respect to the PPM order on both n_a as well as the background noise strength n_b . The actual dependence has been depicted in Fig. 3(a). Assuming for simplicity that the optical pulse employed in the PPM format has a rectangular shape filling the entire time bin with duration equal to B^{-1} , the peak power requirement to attain the optimal performance reads:

$$P_{\text{peak}}^* = B \cdot \eta_{\text{tot}}^{-1} \cdot h f_c \cdot n_s^*(n_a, n_b), \quad (15)$$

where η_{tot} is the overall link transmission efficiency including detection losses defined in Eq. (1), $h f_c$ is the energy of a single photon at the carrier frequency, and $n_s^*(n_a, n_b)$ is the optimal detected pulse energy shown in Fig. 3(b).

The link range r enters Eqs. (14) and (15) through the parameters η_{tot} and n_a , both defined in Eq. (1). As a numerical example, we have taken the transmitter optical power $P_{\text{tx}} = 4$ W, the link bandwidth $B = 2$ GHz, the carrier frequency $f_c = 2 \cdot 10^5$ GHz, and the transmitter and the receiver antenna diameters respectively $D_{\text{tx}} = 0.22$ m and $D_{\text{rx}} = 11.8$ m. For this set of parameters, the attainable information rate R^* , the optimal PPM order M^* , and the required peak power P_{peak}^* are shown in Fig. 5 with solid lines as a function of the link range expressed in astronomical units (AU) for several values of the background noise parameter n_b . For short ranges, below approximately 0.2 AU the performance of the link is limited by the available bandwidth. In this regime the information rate can be characterized by the expression for the noise-free model, given by $B \cdot M^{-1} \log_2 M$. The optimal performance is achieved by the ternary PPM format with $M = 3$, which gives a slightly higher value of mutual information $M^{-1} \log_2 M \approx 0.528$ bit/bin compared to either binary ($M = 2$) or quaternary ($M = 4$) formats for which mutual information is 0.5 bit per time bin.

For ranges beyond several AU, the information rate R^* in the complete decoding scenario shown in Fig. 5(a) exhibits a favorable dependence with the distance r following r^{-2} scaling analogous to the scaling of the detected signal power. This behavior stems from the fact that for diminishing signal power the photon information efficiency $\text{PIE}^*(n_a, n_b)$ in Eq. (14) approaches the constant value PIE^{as} depending only on the noise strength n_b , and the link range r enters the right hand side of Eq. (14) only through n_a . Achieving this performance requires the implementation of extremely high PPM orders, as seen in Fig. 5(b). The required PPM order is given by $M^* = n_s^*(n_a, n_b)/n_a$ and for large distances it scales as r^2 , as in this regime the optimal detected pulse energy $n_s^*(n_a, n_b)$ becomes only a function of the noise strength n_b . The

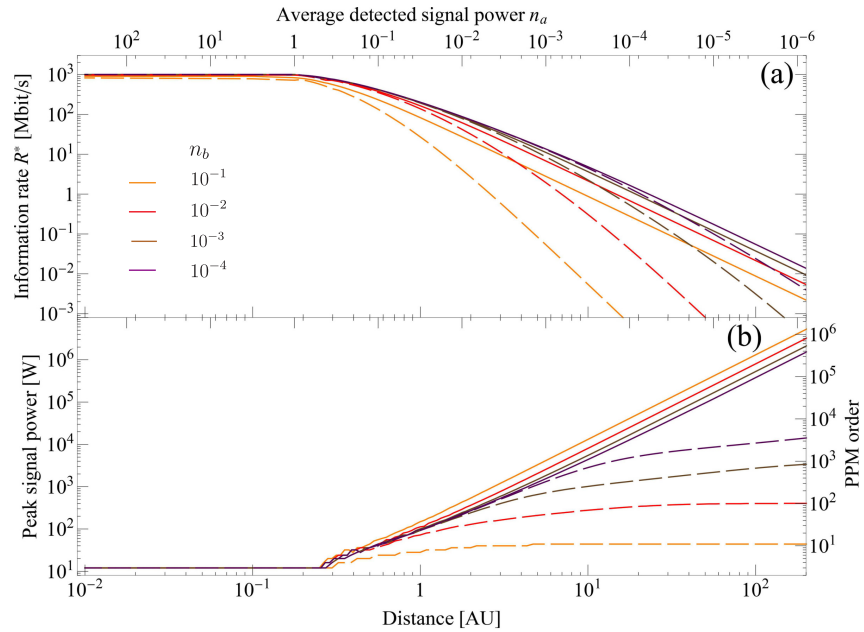


Fig. 5. (a) The maximum information rate R^* of a PPM link as function of the distance r (bottom scale) and the equivalent average detected signal power n_a (top scale) for complete decoding (solid lines) and simple decoding (dashed lines) and several values of the background noise power n_b color-coded according to the legend. The system parameters are: carrier frequency $f_c = 2 \cdot 10^5$ GHz; bandwidth $B = 2$ GHz; transmitter power $P_{tx} = 4$ W; transmitter and receiver antenna diameters $D_{tx} = 0.22$ m and $D_{rx} = 11.8$ m respectively; detector efficiency $\eta_{det} = 0.025$. The distance r is specified in AU units, $1\text{ AU} \approx 1.5 \cdot 10^8$ km. (b) The peak signal power (left scale) and the corresponding PPM order (right scale) required for the optimal operation of the PPM link.

same scaling is exhibited by the peak power P_{peak}^* evaluated according to Eq. (15) and shown in Fig. 5(b).

A more complete analysis of a PPM link would need to include the effects of the detector dead time. However, current superconducting nanowire detectors can have recovery time reduced down to several nanoseconds [21], which corresponds to just few tens of time bins for an exemplary 2 GHz link. For PPM frames substantially longer than this figure and the probability of a background count over the dead time window much less than one the impact of the detector dead time should be minor, as actual light pulses will still have a good chance to produce counts. Another potential problem is the necessity to generate the signal in the form of infrequent strong light pulses to attain the r^{-2} scaling of the information rate. This may lower the overall electrical-to-optical power conversion efficiency of the transmitter module, which is essential for downlink space communication. This issue can be resolved by the use of recently proposed structured optical receivers [15–17]. The basic idea is to generate the optical signal with evenly distributed instantaneous optical power in the form of carefully designed phase or phase-and-polarization patterns which enable one to concentrate temporally the signal energy after transmission using optical interference. Such schemes with quasi-cw optical signals can achieve the efficiency of the PPM format at the expense of a more complicated construction and operation of the receiver. However, these are secondary considerations for downlink transmission of data which becomes the main bottleneck in deep-space communication.

The results obtained for the complete decoding strategy are juxtaposed in Fig. 5 with the

simple decoding scenario depicted with dashed lines. Most importantly, for long ranges the attainable information rate exhibits disadvantageous r^{-4} scaling with the distance. This behavior can be easily understood by inserting in Eqs. (14) and (15) in lieu of PIE^* and n_s^* the asymptotic expressions for $\text{PIE}^{(1)}$ and $n_s^{(1)}$ derived respectively in Eqs. (12) and (13). Because $\text{PIE}^{(1)}$ is linear in n_a , the information rate exhibits quadratic scaling with n_a implying r^{-4} dependence on the distance. On the other hand, the optimal PPM order tends to a constant value for large distances and so does the peak power. The numerical difference between complete and simple decoding is significant, for example at $r = 10$ AU and the background noise strength $n_b = 10^{-1}$ complete decoding allows one to increase the information rate by a factor of hundreds.

6. Conclusions

We have analyzed the range dependence of a noisy optical communication link employing the PPM format and a Geiger-mode photon counting detector, which produces a binary click or no-click outcome in each elementary time bin. Under a fixed average signal power constraint, the attainable system performance, quantified using Shannon information, dramatically depends on the adopted decoding strategy. In the complete decoding scenario, when information is retrieved from all detection events including sequences containing multiple clicks within one PPM frame, it is in principle possible to achieve r^{-2} scaling of the information rate with the distance, i.e. the rate becomes directly proportional to the detected signal power. However, reaching the optimum requires a careful adjustment of the PPM order depending on the operating point of the system. The optimal PPM order grows as r^2 with the covered distance. The resulting demands on the peak-to-average power ratio of the laser light source in the PPM transmitter can be in principle bypassed by resorting to other modulation formats with a scalable order, such as frequency shift keying [22], or concentrating optical energy in the time domain after transmission with the help of structured optical receivers [15–17].

Appendix

In order to derive the lower bound on the photon information efficiency $\text{PIE}^* = \max_M(I^{(M)}/n_a)$ in the complete decoding scenario it will be helpful to resort to an alternative form of the mutual information $I^{(M)}$. Let us denote the count sequence within one PPM frame as $y_1 y_2 \dots y_M$, where $y_j = 0$ denotes no detector click in the j th time bin, while $y_j = 1$ labels a click in that bin. Further, let $p(y|0)$ with

$$p(0|0) = 1 - p_b, \quad p(1|0) = p_b \quad (16)$$

be the conditional no-click and click probabilities for an empty time bin and $p(y|1)$ with

$$p(0|1) = 1 - p_c, \quad p(1|1) = p_c \quad (17)$$

denote analogous probabilities for a bin containing the light pulse. Because all PPM symbols are equiprobable and differ only by the position of the light pulse, mutual information for the complete set of count sequences can be written as

$$I^{(M)} = -\frac{1}{M} \sum_{y_1, y_2, \dots, y_M=0,1} p(y_1|1)p(y_2|0)\dots p(y_M|0) \log_2 \left[\frac{1}{M} \left(1 + \frac{p(y_1|0)}{p(y_1|1)} \sum_{j=2}^M \frac{p(y_j|1)}{p(y_j|0)} \right) \right]. \quad (18)$$

The convexity of the function $-\log_2(ax + b)$ in the argument $x > 0$ for positive a and b allows one to apply Jensen's inequality to individual summations over parameters y_2, y_3, \dots, y_M which yields

$$I^{(M)} \geq -\frac{1}{M} \sum_{y=0,1} p(y|1) \log_2 \left[\frac{1}{M} \left(1 + \frac{p(y|0)}{p(y|1)} (M-1) \right) \right]. \quad (19)$$

The right hand side can be written in terms of the relative entropy defined in Eq. (8) as

$$I^{(M)} \geq \frac{1}{M} D(p_c || (1 - M^{-1})p_b + M^{-1}p_c) \quad (20)$$

where we have returned to notation used in the main text. Let us note that the right hand side in the above equation is identical with the second term on the right hand side of Eq. (7). Eq. (20) implies that $\text{PIE}^* \geq D(p_c || (1 - M^{-1})p_b + M^{-1}p_c) / (Mn_a)$ for any M . Let us now insert $M = n_s^{\text{as}}/n_a$, where n_s^{as} is the value maximizing the right hand side of Eq. (9). This yields:

$$\text{PIE}^* \geq \frac{1}{n_s^{\text{as}}} D(p_c^{\text{as}} || (1 - n_a/n_s^{\text{as}})p_b + n_a p_c^{\text{as}}/n_s^{\text{as}}). \quad (21)$$

where p_c^{as} is evaluated for n_s^{as} . Because relative entropy is continuous, in the limit $n_a \rightarrow 0$ one has $\text{PIE}^* \geq D(p_c^{\text{as}} || p_b)/n_s^{\text{as}}$. Together with Eq. (9), the above inequality implies that PIE^{as} is the asymptotic value of photon information efficiency also for the optimized PPM format.

Funding

TEAM programme of the Foundation for Polish Science co-financed by the European Union under the European Regional Development Fund.

Acknowledgments

We acknowledge insightful discussions with C. Heese, M. Jachura, and M. Srinivasan.

References

- W. D. Williams, M. Collins, D. M. Boronson, J. Lesch and A. Biswas, "RF and optical communications: a comparison of high data rate returns from deep space in the 2020 timeframe," NASA/TM-2007-214459, NASA Glenn Research Center, Cleveland, Ohio, 1–16 (2007).
- H. Hemmati, *Deep-Space Optical Communication* (Wiley, 2005) Chap. 4.
- A. Waseda, M. Sasaki, M. Takeoka, M. Fujiwara, M. Toyoshima and A. Assalini, "Numerical evaluation of PPM for deep-space links," *J. Opt. Commun. Netw.* **3**(6), 514–521 (2011).
- S. Guha, J. L. Habif and M. Takeoka, "Approaching Helstrom limits to optical pulse-position demodulation using single photon detection and optical feedback," *J. Mod. Opt.* **58**(3), 257–265 (2011).
- L. Rizzo, "Effective erasure codes for reliable computer communication protocols," *ACM SIGCOMM Computer Communication Review* **27**(2), 24–36 (1997).
- V. Giovannetti, R. Garcia-Patron, N. J. Cerf and A. S. Holevo, "Ultimate classical communication rates of quantum optical channels," *Nat. Phot.* **8**, 796–800 (2014).
- S. Dolinar, K. M. Birnbaum, B. I. Erkmen and B. Moision, "On approaching the ultimate limits of photon-efficient and bandwidth-efficient optical communication," in *Proceedings of the IEEE International Conference on Satellite Optical Systems and Applications (ICSOS)* (IEEE 2011), pp. 269–278.
- Y. Kochman, L. Wang, and G. W. Wornell, "Toward photon-efficient key distribution over optical channels," *IEEE Trans. Inf. Theory* **60**(8), 4958–4972 (2014).
- M. Jarzyna, P. Kuszaj and K. Banaszek, "Incoherent on-off keying with classical and non-classical light," *Opt. Express* **23**(3), 3170–3175 (2015).
- H. W. Chung, S. Guha and L. Zheng, "On capacity of optical communications over a lossy bosonic channel with a receiver employing the most general coherent electro-optic feedback control," *Phys. Rev. A* **96**, 012320 (2017).
- M. Toyoshima, W. R. Leeb, H. Kunimori and T. Takano, "Comparison of microwave and light wave communication systems in space applications," *Optical Engineering* **46**(1), 015003 (2007).
- B. Moisson and W. Farr, "Range dependence of the optical communications channel," IPN Progerss Report 42–199 (2014).
- J. G. Proakis and M. Salehi, *Communication systems engineering* (Prentice-Hall, Inc., 1994) pp. 11.
- T. M. Cover and J. A. Thomas, *Elements of Information Theory* (Wiley, 2006), Chap. 8.
- S. Guha, "Structured optical receivers to attain superadditive capacity and the Holevo limit," *Phys. Rev. Lett.* **106**(24), 240502 (2011).
- M. Rosati, A. Mari and V. Giovannetti, "Multiphase Hadamard receivers for classical communication on lossy bosonic channels," *Phys. Rev. A* **94**(6), 062325 (2016).
- K. Banaszek and M. Jachura, "Structured optical receivers for efficient deep-space communication," in *Proceedings of the IEEE International Conference on Satellite Optical Systems and Applications (ICSOS)* (IEEE 2017), pp. 176–181.

18. P. L. Kelley and W. H. Kleiner, "Theory of electromagnetic field measurement and photoelectron counting," *Phys. Rev.* **136**(2A), A316–A334 (1964).
19. M. Jarzyna, W. Zwoliński, M. Jachura and K. Banaszek, "Optimizing deep-space optical communication under power constraints," *Proc. SPIE 10524 Free-Space Laser Communication and Atmospheric Propagation XXX*, 105240A (15 February 2018).
20. S. Verdu, "On channel capacity per unit cost," *IEEE Trans. Inf. Theor.* **36**(5), 1019–1030 (1990).
21. D. Rosenberg, A. J. Kerman, R. J. Molnar, and E. A. Dauler, "High-speed and high-efficiency superconducting nanowire single photon detector array," *Opt. Express* **21**(2), 1440–1447 (2013).
22. S. J. Savage, B. S. Robinson, D. O. Caplan, J. J. Carney, D. M. Boroson, F. Hakimi, S. A. Hamilton, J. D. Moores, and M. A. Albota, "Scalable modulator for frequency shift keying in free space optical communications," *Opt. Express* **21**, 3342–3353 (2013).